Human impacts and bistability of forest-savanna in Africa

Thesis submitted in the partial fulfilment of the requirements of the BS-MS dual degree program at IISER, Pune

Prashastha Mishra

20131137

Biology Division, IISER Pune

M.S. Thesis

Under the supervision of
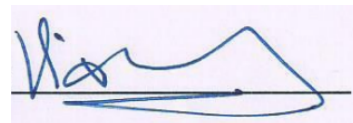
Dr. Vishwesha Guttal

Centre for Ecological Sciences

Indian Institute of Science

CERTIFICATE

This is to certify that this dissertation entitled "**Human Impacts and Bistability of Forest-Savanna in Africa**" towards the partial fulfilment of the BS- MS dual degree programme at the Indian Institute of Science Education and Research, Pune represents research carried out by **Prashastha Mishra** at the Indian Institute of Science, Bengaluru under the supervision of **Dr. Vishwesha Guttal**, Assistant Professor, Centre for Ecological Sciences during the academic year 2017-2018.

Prashastha Mishra

BS-MS Dual Degree Student

IISER, Pune

19th March, 2018

Dr. Vishwesha Guttal

Assistant Professor,

Centre for Ecological Sciences,

Indian Institute of Science

DECLARATION

I hereby declare that the matter embodied in the report entitled "**Human Impacts and Bistability of Forest-Savanna in Africa**" are the results of the investigations carried out by me at the Centre for Ecological Sciences, Indian Institute of Science, under the supervision of **Dr. Vishwesha Guttal** and the same has not been submitted elsewhere for any other degree.
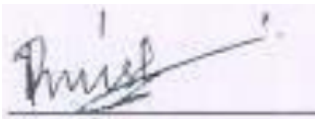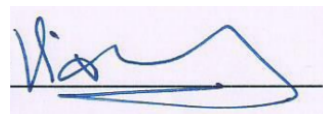
Prashastha Mishra

BS-MS Dual Degree Student

IISER, Pune

19th March, 2018

Dr. Vishwesha Guttal

Assistant Professor,

Centre for Ecological Sciences,

Indian Institute of Science

Abstract

Bimodality in the distribution of tropical tree cover at intermediate environmental conditions is cited as evidence for the presence of bistability in the forest-savanna system. However, bimodality can also emerge because of human activities that cause changes in tree cover, such as the deforestation resulting from expansion in settlements, agricultural and pasture lands. Also, the impact of such activities on tree cover can persist beyond the site of disturbance. Here, I study the relation between human influence and tree-cover bimodality in sub-Saharan Africa, in order to draw conclusions regarding the vegetation dynamics prevalent in the region. I divide remote-sensed vegetation data into regions with low and high degree of human influence. In addition, I devise an environmental predictor of tree cover using relevant climatic and edaphic variables. It is hypothesized that a higher extent of bimodality will be observed in regions with high human influence, because of bimodality arising from human activities, as opposed to bistability. The results show that bimodality is found in regions with both high and low human impacts. However, the extent of bimodality is lower in the regions with low human influence. This indicates that while bistability is restricted to smaller spatial extents than previously assumed, it is common across sub-Saharan Africa, regardless of the presence of human influence.

List of Figures

List of Tables

Acknowledgements

To Dr. Vishwesha Guttal, for being such a patient and perceptive supervisor. I thank him for accepting me as his student and providing invaluable inputs about the project. Beyond his help on this project, I also thank him for his insights on science itself, which helped shape my understanding of it.

To Dr. Krishnapriya Tamma, whose suggestions helped me more than words can describe. I thank her for her patience in lending an ear to my questions, to my ideas and to my unforgivable attempts at humour. It was she who would patiently probe me, ensuring that I asked the right questions and approached them in a logical manner.

To all the people in TEE-lab, for their kindness and endless enthusiasm for science. It was the year I spent in this lab that opened me up to the excitement of doing science, convincing me to pursue science further. I credit this decision to the experience collectively provided by TEE-lab.

To IISER and its faculty, for more things than I can mention in this short space. IISER shaped my life, views and nature more profoundly than I could have imagined. This is greatly due to the education I received here, with its unique emphasis on multi-disciplinary research. I am grateful to all the faculty members, especially the faculty in the Department of Biology, for providing me with knowledge and for inspiring me to do science. A special thanks to Dr. Deepak Barua and Dr. Sutirth Dey for their mentorship and courses, which led me to discover ecology and evolutionary biology.

To my friends, for making the past five years a succession of moments worth remembering forever. I have been lucky to have a peer group that helped me grow both intellectually and emotionally. I thank them for all the discussions we had, on matters mundane and meaningful.

To my late brother and father, for their love and support, which has continued to outlive them.

To my pillar, my North Star - my mother. I thank her for her unwavering faith in me, for giving me all the freedom to pursue my dreams, for everything.

Thank you!

1 Introduction

Environmental conditions, such as climate, nutrient levels, grazing pressure, etc., can change over time. Many ecosystems show a smooth response to such trends in environmental conditions (Fig. 1a). However, in certain cases, when environmental conditions exceed a particular threshold, an ecosystem may undergo an abrupt shift to a contrasting state (Scheffer et al., 2001) (Fig. 1b). Such shifts in the state of an ecosystem are termed 'catastrophic regime shifts' or 'critical transitions'. Critical transitions are difficult to predict, as the system registers little to no change in response to altered environmental variables prior to the threshold, or the 'tipping point'. Additionally, such ecosystems demonstrate hysteresis, i.e., the tipping point for a transition from one state (P1) to another is not the same as the tipping point for a transition in the opposite direction (P2). Ecosystems that demonstrate such dynamics are said to be bistable, i.e., they can occur as two alternative stable states.
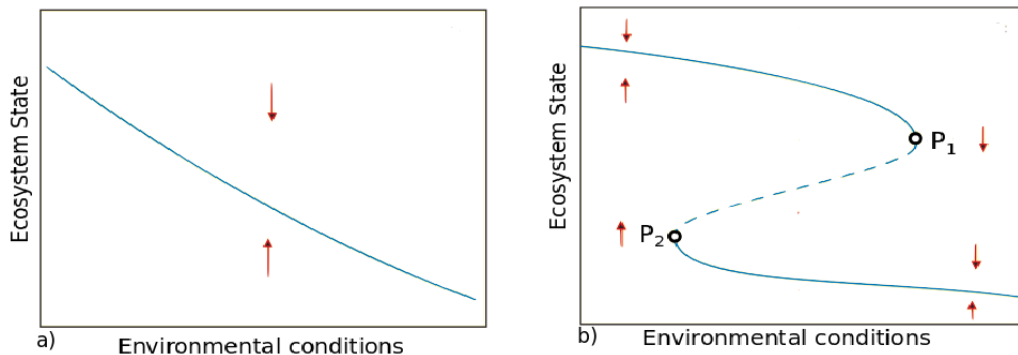

Figure 1: Possible responses of an ecosystem to changes in environmental conditions. In (a), the ecosystem system responds linearly, while in (b), it undergoes a sudden shift in state when environmental conditions are beyond certain thresholds

The presence of bistability has been demonstrated in a number of ecosys-

tems. For instance, based on changes in nutrient loads, shallow lakes can shift between two alternative stable states - an oligotrophic state characterised by dominance of aquatic vegetation, and a eutrophic state characterised by algal dominance (Scheffer et al., 1993). In addition, it has been reported that much of the area that now constitutes the Sahara desert had significantly higher vegetation cover, which underwent a critical transition to deserted state approximately 5000 years ago, precipitated by changes in climate-vegetation feedbacks (Hoelzmann et al., 1998; Jolly et al., 1998; Brovkin et al., 1998). Similar dynamics have been reported to be found in coral reefs (Knowlton, 1992), oceans (Hare and Mantua, 2000), tropical forests and savanna (Staver et al., 2011a).

Since transitions between alternative stable states can lead to significant losses in ecosystem services (Scheffer et al., 2001), it becomes important to recognise ecosystems where bistability is present. It is possible to ascertain the existence of bistability by observing shifts between the alternative stable states as environmental conditions change over time. This approach has helped establish bistability in multiple cases, such as in shallow lakes (Scheffer et al., 1993) and marine ecosystems (Hare and Mantua, 2000). However, this approach requires long-term temporal data, which can often present a challenge, especially for large-scale studies. In such cases, temporal data can be substituted with spatial data to study changes in the ecosystem state with environmental conditions. In bistable systems, both the alternative states co-occur in the range of environmental conditions spanning the tipping points. Thus, over this range of environmental conditions, the state variable (e.g., turbidity of lake, or vegetation cover) has a bimodal distribution (Fig. 2). Since it is difficult to directly demonstrate the presence of bistability in most ecosystems, bimodality in the spatial distribution of a state variable is often presented as evidence of bistable dynamics.

Recent analyses of remote-sensed tree cover data at continental scales
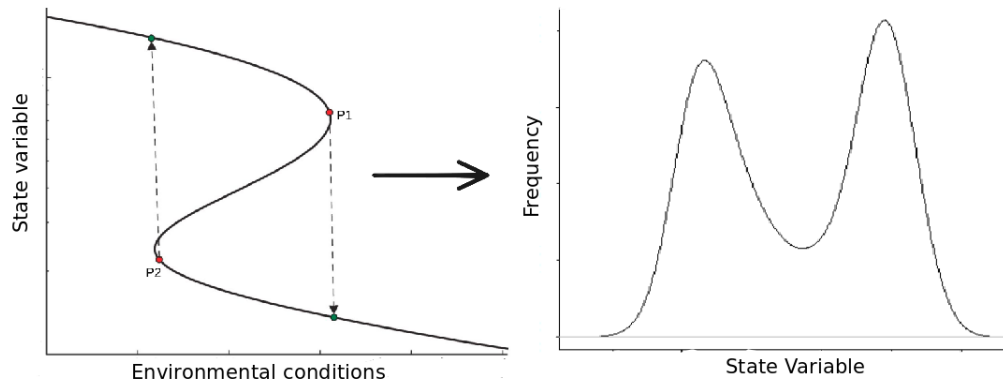
Figure 2: Co-occurence of alternate states over environmental conditions ranging from P1 to P2 gives rise to bimodality in the state variable over that range

have yielded a bimodal distribution of tree cover over intermediate ranges of rainfall, which has been claimed to suggest the presence of alternative stable states in tropical vegetation, i.e., forest and savanna (Hirota et al., 2011; Staver et al., 2011b). This bistability has been linked to fire-tree cover feedbacks in the tropics (Staver et al., 2011a,b). Fire can spread across a connected grassy layer below a certain threshold of tree cover, typically found in savannas. Below this tree-cover threshold, fire leads to opening of the canopy, which promotes even greater spread of fire. No such positive feedback can exist above the threshold, as high tree cover acts to limit fire spread. These feedbacks act to maintain tree cover levels against a climatic backdrop - low rainfall supports savanna, while high rainfall results in forests. At an intermediate range of rainfall, forests and savanna co-exist, which manifests as bimodality in the distribution of tree cover.

However, simulations of dynamical models of vegetation have shown that the rainfall range for which hysteresis occurs can be inflated by spatial heterogeneity in the environment (Nes et al., 2014). Spatial heterogeneity in external variables, such as soil properties, topography and degree of

human influence can lead to expansion in the range of rainfall for which bimodality in tree cover is observed. Thus, the inferred range of bimodality might be higher than bimodality resulting from bistability in vegetation dynamics. In such a case, bistability could be restricted to lower extents than previously claimed.

Humans directly impact vegetation patterns through deforestation, which can introduce bimodality in regions with previously unimodal tree cover. While previous studies acknowledge the effect of anthropogenic factors on tropical vegetation dynamics, most have sought to establish bistability by directly excluding sites of human activities, such as settled areas and agricultural lands (Staver et al., 2011b; Staal et al., 2016). However, human influence can persist beyond the site of such activities (Fig. 3) and lead to changes in tree cover. Not accounting for such human impacts can lead to erroneous inference of bistability in regions where the bimodality arises from anthropogenic disturbances, rather than hysteresis. In addition, this could also hinder the correct estimation of tipping points for critical transitions between alternative states.

In a 2017 study, Wuyts et al. sought to determine the impact of humans in relation to forest-savanna bistability in the Amazonian region. They analysed vegetation data separately for regions affected by human presence and regions that are relatively unperturbed by humans. The extent of bimodality was found to be higher in the regions close to human presence, which implies that human activities can give rise to bimodality. In such a case, bistability in Amazonia is restricted to a smaller spatial extent than previously thought.

In Africa, forest and savanna have been claimed to represent alternative stable states, based on the observation of bimodal tree cover distribution within an intermediate range of rainfall (Staver et al., 2011b; Hirota et al., 2011). However, the forest-savanna system supports a large section of the African population. It is likely that human activities have introduced bi-

modality in the region, independent of bistability in the system. If this is indeed the case, regions with a high degree of human influence can be expected to have a larger range of environmental conditions for which forest and savanna co-exist, as compared to regions with low human influence.

This study aimed to examine the influence of humans on bimodality and bistability in the African forest-savanna system. The study area of sub-Saharan Africa, was broadly divided into human-affected and natural regions, corresponding to high and low degree of human influence, respectively. Using spatial data for a number of environmental variables that are thought to influence tree cover at continental scales, such as mean annual rainfall, seasonality, temperature and soil properties (Greve et al., 2011; Oliveras and Malhi, 2016), a composite environmental predictor (CEP)
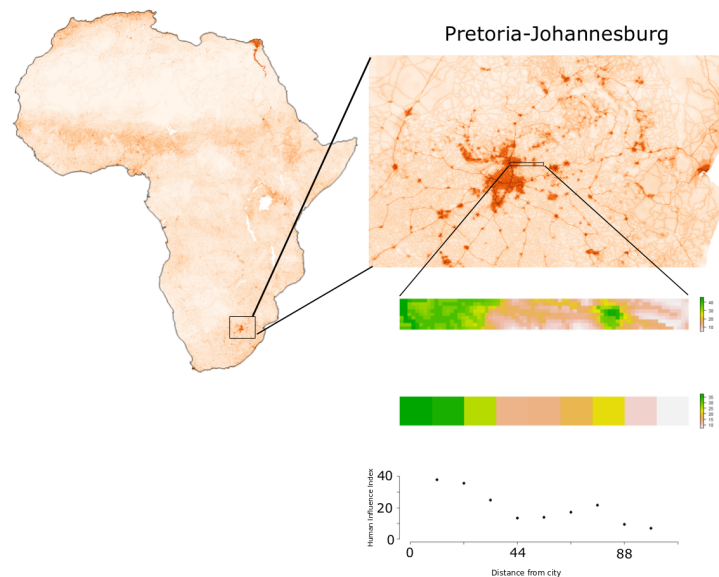
Figure 3: Impacts of humans on tree cover can persist beyond the site of their presence. As an example, the human influence index (a measure of human impact) remains high even as one moves 44 km away from the highly-populated Pretoria-Johannesburg region in South Africa

of tree cover was derived. Following this, the extent of bimodality in the human-affected and natural regions were compared, in order to ascertain the influence of humans on tree cover. While bimodality in tree cover was observed to exist in both natural and human-affected regions, the extent of bimodality was lower in the natural regions. These results are in agreement with the hypothesis that human impacts would cause bimodality to be more frequent in the human-affected areas. Therefore, bistability is arguably restricted to smaller extents than previously assumed. However, the existence of bimodality in both natural and human-affected regions suggest that bistability is ubiquitous in the forest-savanna system of Africa.

2 Methods

2.1 Study Area

The study was restricted to the region spanning sub-Saharan Africa (Fig. 4). Using Globcover 2010, a global dataset on land cover, regions corresponding to land cover classes such as water bodies and wetlands (Bontemps et al., 2011) were excluded from the analysis.
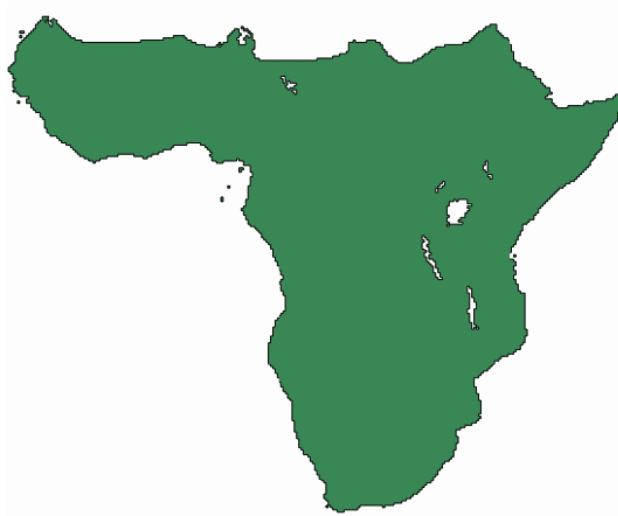
Figure 4: Map of Study Area

2.2 Tree Cover

Vegetation indices are widely used as proxies for tree cover. For this study, data regarding vegetation indices for the study region was obtained from the satellite-derived MODIS VI (MOD13) product suite (Huete et al.), via the Google Earth Engine (Gorelick et al., 2017). The MODIS (Moderate Resolution Imaging Spectrometer) VI products provide gridded vegetation maps at each 16-day interval. Two separate products are derived globally

- NDVI (Normalised Difference Vegetation Index) and EVI (Enhanced Vegetation Index). This analysis was based on the EVI products, since EVI is more sensitive to differences in high tree-cover regions and also incorporates corrections for aerosol concentration levels, which can introduce significant noise to the signal. The study utilised EVI data from the year 2010. Additionally, in order to mitigate any systematic errors in measurement caused by cloudiness, only the data corresponding to the dry months of June-July was considered.

2.3 Environmental Variables

Environmental variables that have previously been reported to be relevant large-scale determinants of forest-savanna distribution were considered in the analysis (Greve et al., 2011; Oliveras and Malhi, 2016; Murphy and Bowman, 2012; Lehmann et al., 2011). Apart from mean annual rainfall, which has been the most frequently used environmental variable in previous studies, the variables included were Markham's Seasonality Index (MSI) for rainfall, mean annual temperature, soil bulk density and the clay, sand and silt content of soil. Through resampling in R, data for each of these variables was adjusted to have a common resolution of 0.25 degrees x 0.25 degrees (approximately 27 sq. km).

2.3.1 Mean Annual Rainfall

Mean annual rainfall is considered to be most important determinant of tree cover (Murphy and Bowman, 2012) and has been used widely in studies of bistability in tropical vegetation (Hirota et al., 2011; Staver et al., 2011a). Thus, it was included among the environmental variables used in the study. Rainfall data was obtained from TRMM (Tropical Rainfall Measuring Mission) 3B42, which is a product derived from merged satellite and rain-gauge estimates of precipitation (Huffman et al., 2007). The 3B42 rain-

Variable	Reference	Original Resolution
Mean Annual Rainfall (MAR).	Huffman et al., 2007	0.25' x 0.25'
Rainfall Seasonality (MSI)	Huffman et al., 2007	0.25' x 0.25'
Mean Annual Temperature (MAT)	Fick and Hijmans, 2017	1 km x 1 km
Subsoil Clay Fraction	Hengl et al. 2017	1 km x 1 km
Subsoil Sand Fraction	Hengl et al. 2017	1 km x 1 km
Subsoil Silt Fraction	Hengl et al. 2017	1 km x 1 km
Topsoil Clay Fraction	Hengl et al. 2017	1 km x 1 km
Topsoil Sand Fraction	Hengl et al. 2017	1 km x 1 km
Topsoil Silt Fraction	Hengl et al. 2017	1 km x 1 km
Topsoil Bulk Density	Hengl et al. 2017	1 km x 1 km

Table 1: Names, references and original resolutions of environmental variables used in the study.

fall estimates have a temporal resolution of 3 hours and spatial resolution of 0.25 x 0.25 degrees. Mean annual rainfall (MAR) is defined as

$$MAR = \frac{1}{y_2 - y_1} \sum_{y=y_1}^{y_2} \sum_{m=1}^{12} p_{y,m} \tag{1}$$

where y_1 and y_2 represent the initial and final years of measurement, while $p_{y,m}$ represents rainfall in month *m* of year *y*. Since the temporal extent of this analysis was from year 2000 to 2010, TRMM rainfall maps were obtained for this period and processed via Google Earth Engine to estimate MAR.

2.3.2 Seasonality

In addition to the annual mean, seasonality in rainfall can also influence tree cover in a region. A high seasonality in rainfall can have twofold consequences - it can reduce tree growth and also encourage fire spread in

the intervening dry months (Lehmann et al., 2011). This study incorporated seasonality in rainfall, estimated as Markham's Seasonality Index (MSI) (Markham, 1970). MSI assumes mean rainfall for each month to be a vector, whose direction is the month in arc units and magnitude is the monthly mean of rainfall. The monthly vectors are then summed and normalised to yield MSI. MSI can take values from 0 to 1, with higher values denoting higher seasonality.

For this analysis, MSI was calculated according to the method formulated by Scheiter et al. (2015):

$$MSI = 100\frac{1}{R}\sqrt{(H_x)^2 + (H_y)^2} \tag{2}$$

where $H_x = \sum_{i=1}^{12} r_i \cos\frac{2\pi\alpha_i}{360}, H_y = \sum_{i=1}^{12} r_i \sin\frac{2\pi\alpha_i}{360}$ and α_i is direction of the vector, i.e., $\alpha_1 = 15, \alpha_2 = 30$ and so on. Mean rainfall was calculated for each month and added vectorially according to this formulation to yield an estimate of rainfall seasonality.

2.3.3 Temperature

Data on annual mean temperature was obtained from WorldClim Version 2 (Fick and Hijmans, 2017), which includes spatially interpolated temperature data from 1970-2000.

2.3.4 Soil Properties

Soil properties such as texture and nutrient availability form another basis of differences between forest and savanna (Murphy and Bowman, 2012). Heterogeneity in nutrient and textural variables could contribute to observed patterns tree cover. However, due to the lack of data on soil nutrient variables at continental scales, only textural variables were incorporated into the study. The soil properties considered for the analysis included bulk

density, clay fraction, sand fraction and silt fraction. Each of these properties were estimated separately for topsoil (0-30 cm) and subsoil (30-100). Data was obtained from SoilGrids (Hengl et al., 2017), a global gridded soil database built from automated compilation of soil profile and remote-sensed data. The SoilGrids database has data on soil properties only at certain standard depths - 0 cm, 5 cm, 15 cm, 30 cm, 60 cm, 100 cm and 200 cm. To derive an average estimate of the soil properties for the entirety of topsoil and subsoil, the trapezoidal method of definite numerical integration was used:

$$\frac{1}{b-a} \int_a^b f(x)dx \approx \frac{1}{2(b-a)} \sum_{k=1}^{N} \frac{x_{k+1} - x_k}{f(x_k) + f(x_{k+1})} \tag{3}$$

where N = number of depths, $x_k = k_{th}$ depth and f(x) = value of soil property at k_{th} depth. From the original resolution of 1 sq. km, the final data was resampled to a resolution of 0.25 x 0.25 degrees (approximately 27 sq. km).

2.4   Composite Environmental Predictor

Most studies rely on the effect of mean annual rainfall on the distribution of tree cover to infer forest-savanna bistability. However, there exist multiple other environmental determinants of tree cover, including edaphic and other climatic variables. Spatial heterogeneity in these variables can enlarge the range of rainfall for which bimodality in tree cover is observed, leading to an overestimation of rainfall-related bimodality. In an effort to minimize this effect of spatial heterogeneity, a composite variable was devised using several climatic and edaphic variables. The climatic variables included mean annual rainfall (MAR), Markham's seasonality index (MSI) for rainfall and mean annual temperature (MAT). Edaphic variables used were bulk density, clay fraction, sand fraction and silt fraction. With the exception of bulk density, each variable was estimated separately for topsoil

and subsoil.

The data for each of these variables was processed as described in the previous section. Each pair of environmental variables were subjected to Pearson's correlation tests. Many variables were found to be highly correlated and inclusion of such correlated variables in the analysis could lead to erroneous inferences.

The composite variable was derived from the mentioned environmental variables using principal component analysis (PCA), performed in R using the RStoolbox package (Leutner and Horning, 2016). A PCA takes in a dataset of multiple linearly correlated variables and transforms them into a new coordinate system, yielding a set of uncorrelated 'principal components'. The procedure reduces the dimensionality of a dataset, while retaining the variation within the data. Thus, a PCA would allow the the set of multiple, correlated variables to be reduced into a few, linearly uncorrelated components. The principal component with the highest variance was then used as the composite variable, henceforth referred to as the 'Composite Environmental Predictor' of tree cover (CEP). Instead of examining the relationship between mean annual rainfall and tree cover, as in previous studies, the effect of CEP on tree cover was analysed in order to draw conclusions about vegetation dynamics in the study area.

Finally, to discern which of the environmental variables contribute most of the variance to the CEP, Pearson's correlation tests were conducted between the CEP and each variable.

2.5   Division of study area into natural and human-affected regions

The Human Footprint (HFP) maps provide information about the pressures exerted by humans in terrestrial regions across the globe (Sanderson et al., 2002; Venter et al., 2016). The maps are compiled with information from

both remote-sensing and bottom-up surveys measuring eight variables, each representing various direct and indirect human pressures on the environment. The eight pressure variables include the following: (1) the extent of built environments, (2) population density, (3) electric infrastructure, (4) crop lands, (5) pasture lands, (6) roads, (7) railways, and (8) navigable waterways. These variables are combined to yield a cumulative indicator of human pressures (Fig. 5), termed the Human Influence Index (HII). High values of HII correspond to areas where anthropogenic impacts are high. Such areas are likely to be undergoing changes from their original state as a result of the human pressure. Conversely, regions with low HII are relatively unaffected by the pressure variables and likely to be in their natural states. Information from most recent Human Footprint dataset, HFP 2009, was used to divide the study area into regions of high and low human influence. The HFP map was truncated to the spatial extent of the study area. Since the original dataset has a resolution of 0.0028 x 0.0028 degrees (approximately, 0.3 sq. km), it was adjusted to a lower resolution of 0.25 x 0.25 degrees, common to the resolution of the other spatial datasets used in the analysis. In addition, the dataset was transformed to the WGS 84 projection, from its original Mercator projection.

The value of Human Influence Index corresponding to the 25th percentile was chosen to be used to separate the study area by degree of human impacts. The value of HII which covers 25 percent of the area under the density curve for was estimated through a Reimann sum (a numerical method of approximation of finite integrals). This value of HII was then used as a threshold to broadly divide the study area according to degree of anthropogenic influence. Pixels with an HII greater than this threshold were designated to be 'human-affected', while those with HII less than or equal to the threshold were included in the 'natural regions'.
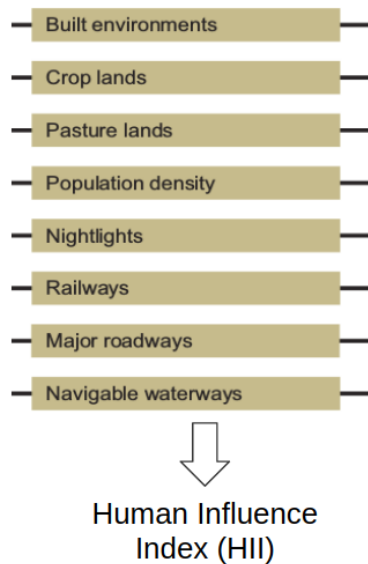
18

Figure 5: Calculation of a cumulative Human Influence Index from individual human pressure variables

2.6 Spatial data

All datasets obtained were in the WGS 84 projections. Each dataset was adjusted to have a common spatial resolution of 0.25 x 0.25 degrees, along with a spatial extent corresponding to the study area of sub-Saharan Africa. Analysis of the data was performed through R (Team, 2000) and qGIS.

2.7 Tree Cover versus CEP Plots

EVI was plotted against CEP separately for natural and human-affected regions, in order to study changes in tree cover with human impacts. For this, the maps corresponding to EVI and CEP were divided into the human-affected and natural areas. Following this, both natural and human-affected areas were divided into multiple "bins", or segments, each spanning 50

PC1 units, i.e., -1550 to 1500, -1500 to -1450, and so on. For each segment, the density plot of tree cover was obtained. The nature of the tree cover distribution in the segments was established according to the following set of rules:

1) The distribution was designated to be bimodal if the modes were separated by more than 1000 units of EVI and were at least 25 percent of each other's height.

2) In case of the occurrence of more than two modes, a mode is disregarded if its height is less than 10% of the height of the largest mode. However, if such a mode is separated by less than 1000 units of EVI and is comparable to the height of the closest mode, a weighted average of the two closely-occurring modes is considered.

3) In case two modes are separated by more than 1000 units of EVI, but are less than 25% of each other's height, the two modes are depicted in the final plot if they are at least 10% of each other's height. However, such a distribution is not designated to be bimodal.

4) In case neither of conditions (1) and (2) are satisfied, the distribution is designated to be unimodal.

The values of the modes were obtained and the nature of the distribution was decided based upon the above rules. Following this, the value of the tree cover modes were plotted for each bin of CEP, i.e., each segment spanning 50 PC1 units. Such plots are henceforth called 'state diagrams'. State diagrams were constructed separately for both natural and human-affected areas. The range of CEP corresponding to bimodality was obtained by estimating the number of segments that continuously have a bimodal distribution of tree cover. This range was then compared for the natural and human-affected regions.
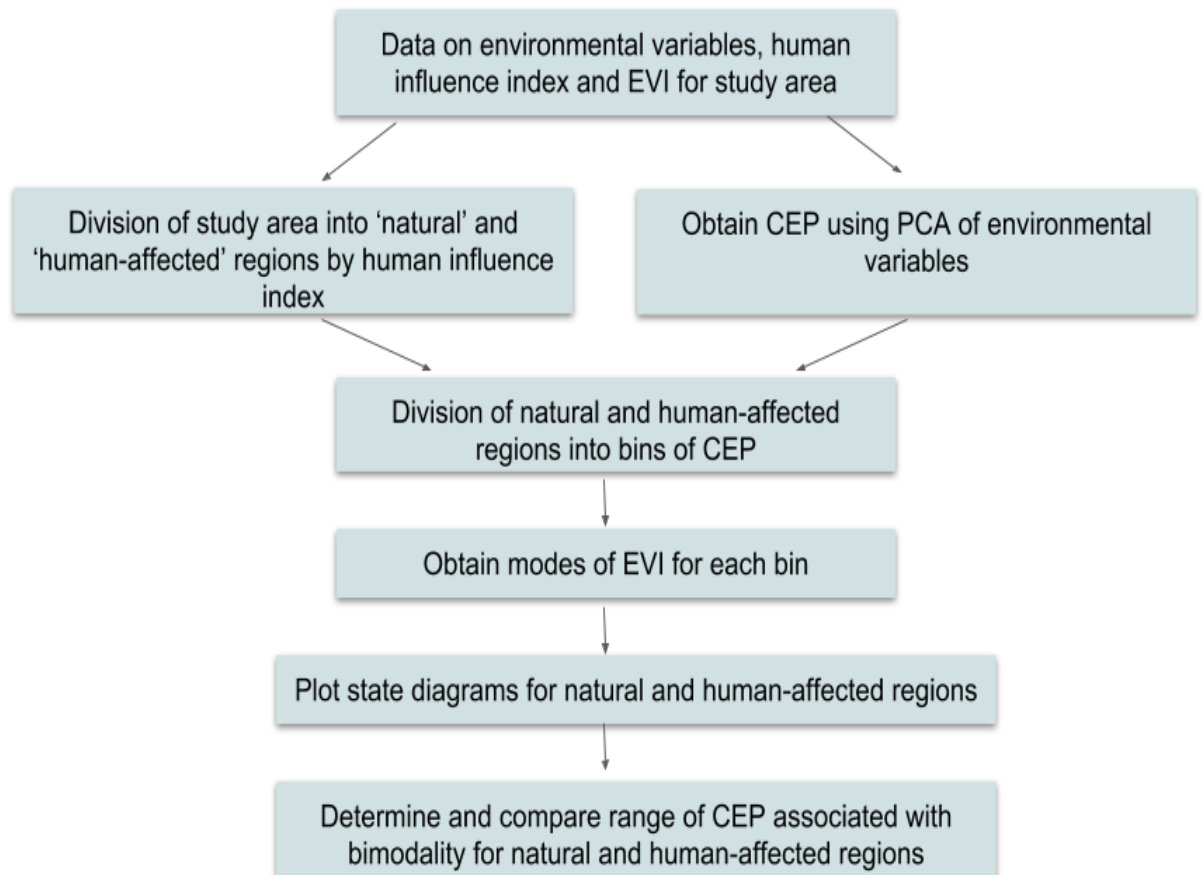
Figure 6: Flowchart of methods used in the analysis.

2.8 Sensitivity Analysis

Any differences in the extent of tree-cover bimodality can potentially be attributed to the the value of HII chosen to separate sub-Saharan Africa into two distinct regions by degree of human impact. To ascertain the role of the choice of this threshold in the results of the study, sensitivity analysis was conducted using two different values of HII to assess any difference in the outcome. The value chosen originally corresponded to the 25th percentile of HII. Values of HII at 15th and 35th percentile were chosen for

the sensitivity analysis. Using Riemann sum, HII was estimated at these percentiles. By taking the value of HII thus obtained as the threshold, the study area was divided into natural and human-affected regions. The extent of bimodality in each was then compared in order to discern any effect of HII on the observations.

In order to further test the efficacy of dividing the study area by the HII at the 25th percentile, a frequency distribution of GlobCover classes was obtained for the 'natural' areas. If the 25th percentile cutoff is sufficiently stringent, the natural areas would have low frequency of occurrence of land cover classes associated with human presence, such as croplands and urban areas.

3 Results

3.1 Division of study area into natural and human-affected regions

The value at the 25th percentile of HII for the study area was found to be 4.3, given the spatial resolution used in the study. As a result, regions with $HII \leq 4.3$ were designated as 'natural', while regions with $HII >$ were designated to be 'human-affected' (Fig. 7).

GlobCover land classes linked to high human influence were found to have a low frequency in the regions deigned to be 'natural' using the above criterion. The frequencies of human-associated land cover classes are listed below in Table 2.
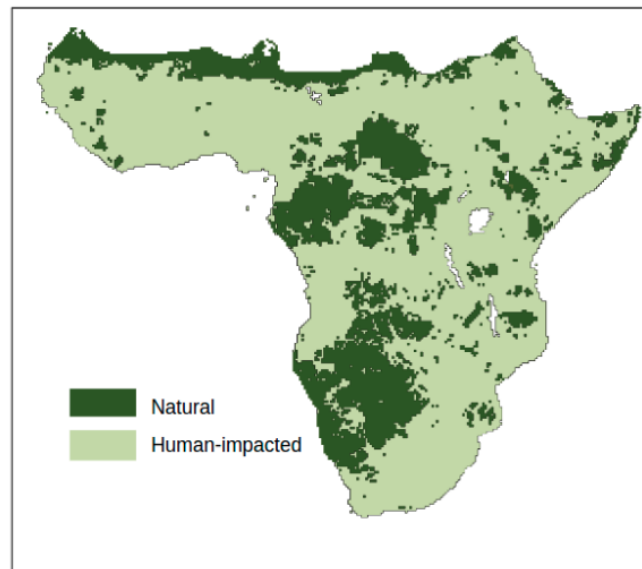

Figure 7: Study area, divided into natural and human-affected regions using an HII of 4.3 as the threshold.

GlobCover Class	Frequency
Croplands (Irrigated)	0
Croplands (Rainfed)	0.0050
Mosaic cropland (50-70%) / vegetation (grassland/shrubland/forest) (20-50%)	0.3830
Mosaic vegetation (50-70%) / cropland (grassland/shrubland/forest) (20-50%)	1.7049
Urban areas (>50%)	0.0059

Table 2: Frequency of human-associated GlobCover land classes in the natural areas, delineated using an HII threshold of 4.3

3.2 Pairwise correlations between environmental variables

Multiple environmental variables of the same class (i.e., climatic or edaphic) were found to be significantly correlated with each other (Table 3).

	MAR	MSI	MAT	Subsoil clay fraction	Subsoil sand fraction	Subsoil silt fraction	Topsoil clay fraction	Topsoil bulk density	Topsoil sand fraction
MSI	-0.0898								
MAT	-0.1464	0.6565							
Subsoil clay fraction	0.6231	-0.1014	-0.0532						
Subsoil sand fraction	-0.5013	0.0074	-0.1248	-0.9351					
Subsoil silt fraction	0.1289	0.1583	0.3936	0.5210	-0.7897				
Topsoil clay fraction	-0.7413	0.2401	0.0796	-0.6788	0.6436	-0.3754			
Topsoil bulk density	0.5327	-0.0673	0.0054	0.9765	-0.9258	0.5394	-0.6512		
Topsoil sand fraction	-0.4361	-0.0212	-0.1804	-0.9048	0.9890	-0.8155	0.6253	-0.9265	
Topsoil silt fraction	0.1716	0.1468	0.3902	0.5467	-0.8071	0.9972	-0.4130	0.5596	-0.8303

Table 3: Pearson's correlation coefficient between environmental variables used in the analysis

3.3 Principal Component Analysis

The first principal component (PC1) accounted for a large fraction of the variance, at 99.4 per cent. Therefore, it was seen fit to be used as the Composite Environmental Predictor (CEP).

Among all the environmental variables considered in the PCA, mean annual rainfall had the highest correlation with the first principal component, i.e., the CEP. Mean annual rainfall correlates highly with CEP (Pearson's correlation coefficient = 0.99, $p < 0.05$). The correlation coefficients for the other climatic and soil variables are listed in Table 4.

Environmental variable	Pearson's correlation
MAR	0.9998
MSI	0.1452
MAT	0.0913
Subsoil clay fraction	-0.6298
Subsoil sand fraction	0.5108
Subsoil silt fraction	-0.1412
Topsoil clay fraction	-0.5408
Topsoil bulk density	0.7512
Topsoil sand fraction	0.4468
Topsoil silt fraction	-0.1837

Table 4: Pearson's correlation coefficient between environmental variables and the composite environmental predictor (CEP)

3.4 Bimodality in natural and human-affected regions

The scatterplots of tree cover versus CEP were generated separately for both natural and human-affected regions (Fig. 8). The incidence of low tree cover was observed to overlap with high tree cover for an intermediate range of CEP in both regions. However, the degree of overlap appears to be larger in the human-affected parts of the study area. The degree of overlap, i.e., the range of CEP with bimodality, was quantitatively estimated through state diagrams, generated through steps described in section 2.7.

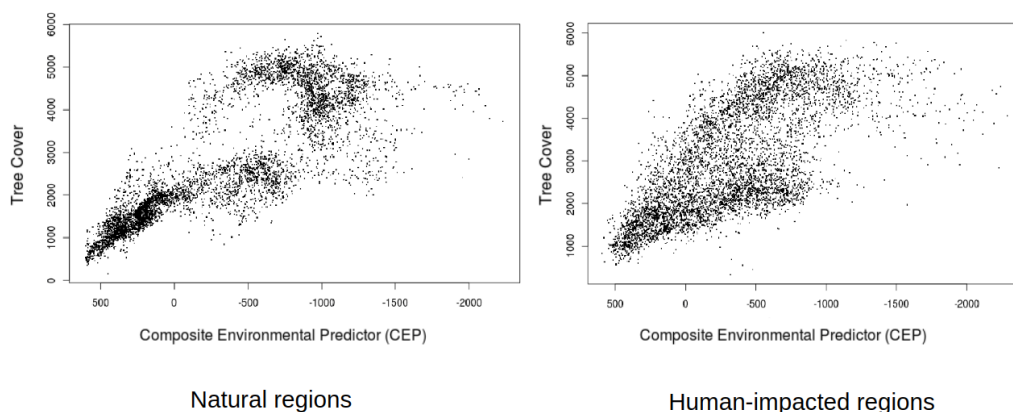Natural regions   Human-impacted regions

Figure 8: Scatterplots of tree cover versus CEP for natural and human-affected regions. The overlap between high and low tree cover is greater in human-affected regions.

A comparison of state diagrams shows that the range of CEP associated with bimodality is higher for human-affected regions. Natural regions show bimodality across 15 segments, i.e., 750 PC1 units, while human-affected regions have a range of bimodality spanning 20 segments, i.e., 1000 PC1 units (Fig. 9).
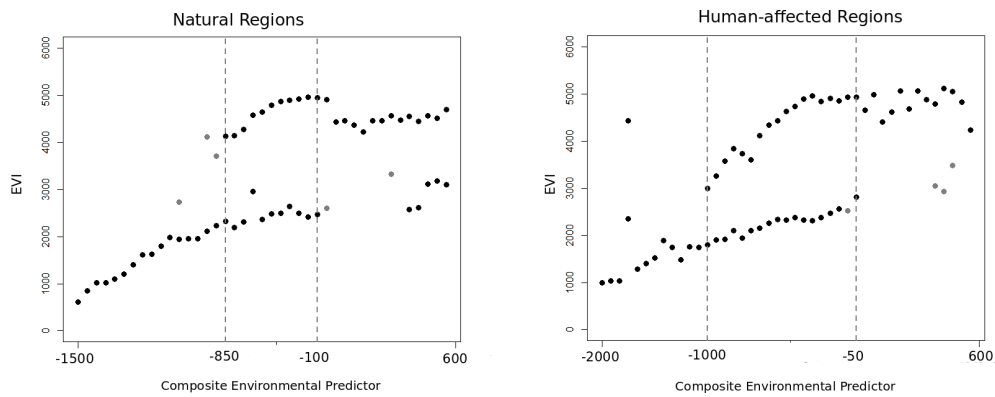
Figure 9: State diagrams for natural and human-affected regions. Bimodality in tree cover occurs over a greater span of CEP values in the human-affected areas.

3.5   Sensitivity Analysis

The study area was divided using HII at 15th, 25th and 35th percentile as threshold and state diagrams were obtained for the natural and human-affected regions, using steps in section 2.7 (Figs. 10-12). Sensitivity analysis indicates that the degree of overlap between high and low tree cover is unaffected by changes in the threshold of HII used to separate the study

Percentile of HII	HII threshold	Range of bimodality in natural regions (PC1 units)	Range of bimodality in human-affected regions (PC1 units)
15	3.1	700	1000
25	4.3	750	1000
35	5	700	1000

Table 5: Results of Sensitivity analysis. The range of value of CEP associated with bimodality remains largely unchanged even as one changes the criterion for division of the study area into natural and human-affected regions.
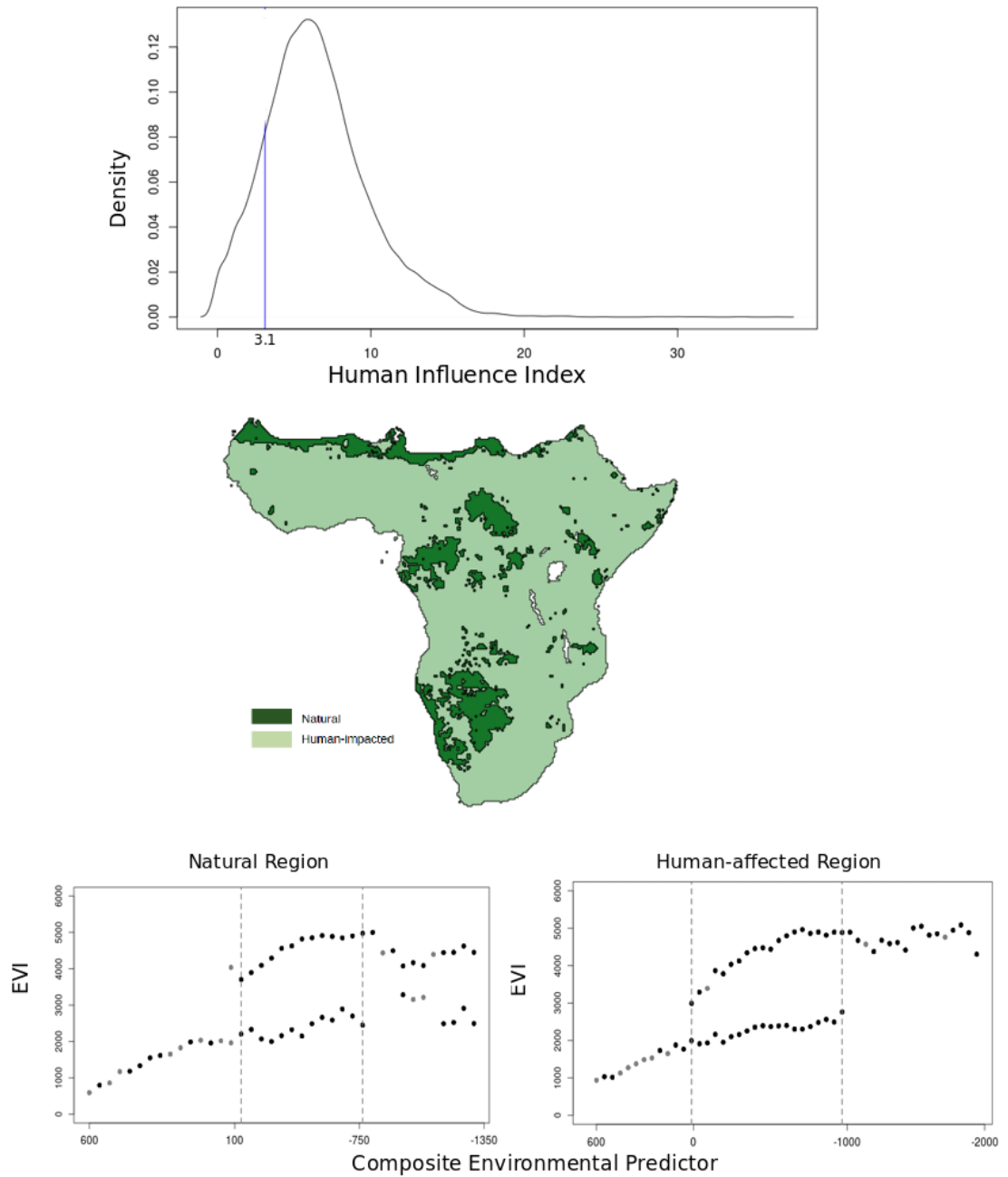
Figure 10: Sensitivity analysis at 15th percentile of HII. The value of HII associated with the 15th percentile of the distribution was found to be 3.1. The study area was divided into natural and human-affected areas using HII = 3.1 as the cut-off. State diagrams were then plotted for both, to determine the range of CEP that shows bimodality. At 15th percentile, bimodality spans 700 and 1000 units of CEP, for the natural and human-affected regions, respectively

28

Figure 11: Sensitivity analysis at 25th percentile of HII. The cut-off for division of the study area into natural and human-affected regions, estimated as the HII at 25th percentile, was found to be at HII = 4.3. Bimodality was found to span 750 and 1000 units of CEP, for natural and human-affected regions, respectively.
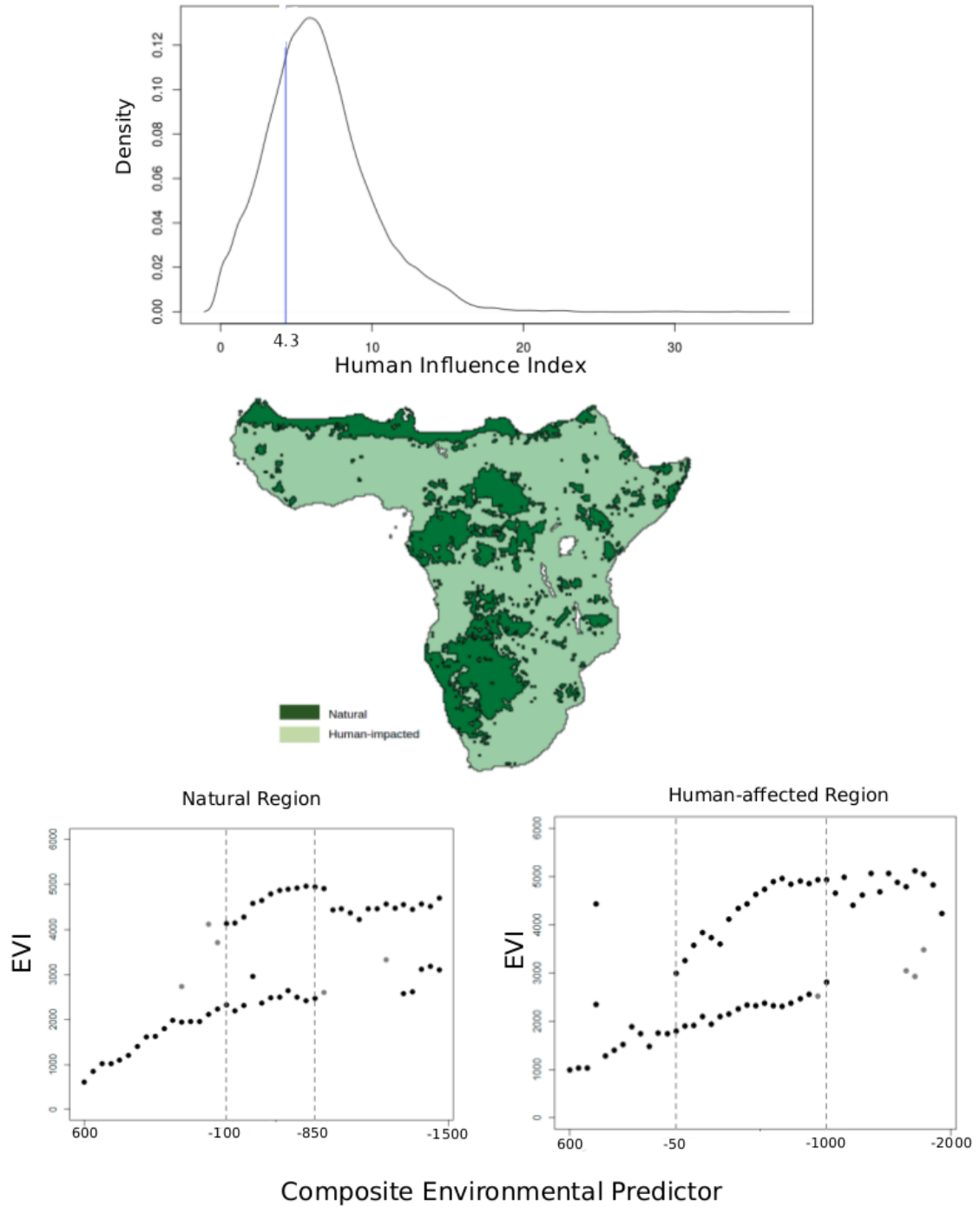
29
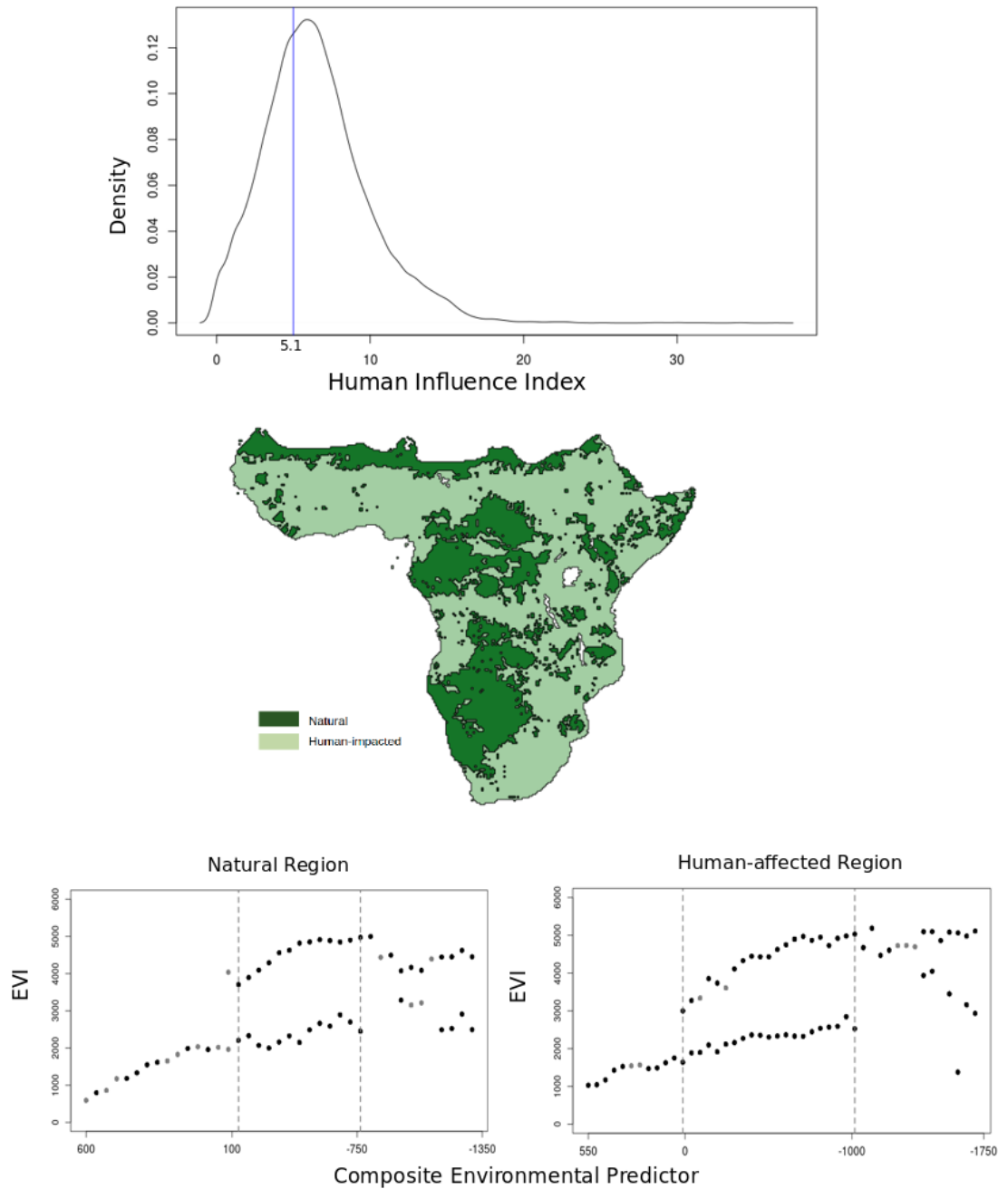
Figure 12: Sensitivity analysis at 35th percentile of HII. The cut-off for division of the study area into natural and human-affected regions, estimated as the HII at 35th percentile, was found to be at HII = 5. Bimodality was found to span 700 and 1000 units of CEP, for natural and human-affected regions, respectively.

area into natural and human-affected regions. The values of CEP corresponding to bimodality showed no significant changes across different criteria for separation of study area into natural and human-affected regions. The range of CEP for bimodality at the different thresholds are listed here in Table 5.

4 Discussion

In this study, I aimed to discern the relation between human impacts and vegetation patterns in sub-Saharan Africa. Studying this relation is crucial because the observed large-scale patterns in the distribution of tree cover have been used as evidence for bistability in the vegetation dynamics. In Africa, continental-scale bimodality in tree cover has been cited in support of bistability (Staver et al., 2011b; Hirota et al., 2011). However, the forest-savanna complex in sub-Saharan Africa is subject to very high levels of human activity, which needs to be taken into account in studies of vegetation dynamics of the region.

A composite environmental predictor (CEP) of tree cover was devised from relevant environmental variables. Mean annual rainfall was found to be the most highly correlated with the CEP, with the loading of other environmental variables being lower. The study area, sub-Saharan Africa, was divided into two parts - highly impacted 'human-affected' areas and 'natural' areas with low human impacts, with the help of information from the Human Footprint Map dataset. Analysis of spatial tree-cover data revealed an overlap in the occurrence of forest and savanna states at intermediate values of the composite environmental predictor. This overlap, or tree-cover bimodality, was found in regions subject to both high and low degrees of human influence. The overlap was observed to be higher in the human-affected regions, in keeping with the expectation that human activities can inflate the presence of bimodality in tree cover. This result is consistent even as the criterion for division into human-affected and natural areas is changed.

The results of the study show that there exists bimodality in forest and savanna states of African tropical vegetation, even after accounting for the confounding effect of spatial heterogeneity in multiple environmental variables. However, the range of environmental conditions that support bi-

modality is larger in regions that are affected to a greater extent by human activities. This is in agreement with previous theoretical findings, which contend that spatial heterogeneity in variables such as human impact can give rise to bimodality (Nes et al., 2014). This implies that the bimodality observed in rainfall-tree cover plots generated from remote-sensed spatial vegetation data (Staver et al., 2011b; Hirota et al., 2011) is at least partly associated with anthropogenic phenomena, as opposed to hysteresis caused by large-scale bistability in the vegetation. This can be interpreted as bistability being restricted to smaller regions than assumed earlier. Nevertheless, the presence of significant bimodality in both natural and human-impacted regions indicates that bistability is pervasive throughout the forest-savanna system studied here.

The results obtained through this analysis are similar to the observations reported by Wuyts et al. (2017), in a study regarding the relation between human impacts and forest-savanna distribution in Amazonia. Based on the observation that bimodality is largely limited to regions close to human-inhabited areas, the authors claimed that a significant portion of bimodality in Amazonian vegetation is attributable to changes in tree cover resulting from human actions, such as logging, or clearing of forests for agricultural or pasture lands. Contrary to this study, however, our results show that even in the 'natural' regions, bimodal tree cover occurs over a fairly large range of environmental conditions. This could be a reflection of the differences in the distribution of human population between Amazonia and sub-Saharan Africa. Population densities, and accordingly, human impacts, increase in a gradient, beginning from the low densities of the forested Amazon basin to high densities in the drier regions, known as *cerrado*. Contrastingly, human impacts occur in a more scattered manner in sub-Saharan Africa, with significant population densities found even near forested areas.

The differences in the extent of bimodality between the natural and

human-affected areas could arise from direct changes to tree cover caused by deforestation or afforestation. In addition, the difference could arise from anthropogenic changes in important determinants of forest-savanna distribution, such as changes in variables related to fire and herbivory. Humans can manipulate fire regimes, potentially altering the vegetation-fire feedbacks crucial for maintaining the vegetation patterns found in a landscape (Oliveras and Malhi, 2016; Archibald et al., 2012). Humans have been known to influence vegetation patterns through fire since prehistoric times, with the record of anthropogenic fire in Africa going back to nearly a million years (Bird and Cali, 1998). It has been reported that the rise in human presence and the accompanying shifts in fire ignition or suppression can result in changes in the key characteristics of fire, such as fire size, intensity, frequency and season (Archibald et al., 2013). Such anthropogenic alterations in fire characteristics could be a reason for the difference in bimodality observed between the natural and human-affected regions. In addition to fire, grazing can significantly shape vegetation patterns in a landscape (Murphy and Bowman, 2012). Introduction of livestock by humans could modify tree cover patterns, either directly, or through fire-herbivory (Archibald et al., 2005), or soil-herbivory feedbacks (Rietkerk et al., 2000). Thus, higher grazing activity could also be a reason for the difference in extent in bimodality between the two classes of human impact. Indeed, predictable differences in fire characteristics and herbivory have been found between the natural and human-affected areas (Tamma et al., in prep).

The study was conducted at a relatively coarse resolution of 0.25'x 0.25', which could have affected the results. Soil properties are known to be relevant at smaller, regional scales (Lehmann et al., 2011). Thus, it is likely that a similar study, done at a higher spatial resolution would have results that better reflect the effect of soil properties on vegetation. In addition, the study relied on spatial vegetation data obtained for a particular year. However, vegetation cover may show changes over time. It

is possible that the results could be affected by such temporal variation in vegetation cover.

Nevertheless, the results suggest that there exists significant bimodality in vegetation cover in the study region, regardless of the presence or absence of humans. Hence, at least for Africa, previous studies that claimed forest-savanna bistability based on the presence of bimodality in tree cover seem to hold true. However, human influence needs to considered alongside tree cover data in order to draw further inferences regarding the nature of vegetation dynamics in an area.

References

Archibald, S., Bond, W., Stock, W., and Fairbanks, D. (2005). Shaping the landscape: fire–grazer interactions in an african savanna. *Ecological applications*, 15(1):96–109.

Archibald, S., Lehmann, C. E., Gómez-Dans, J. L., and Bradstock, R. A. (2013). Defining pyromes and global syndromes of fire regimes. *Proceedings of the National Academy of Sciences*, 110(16):6442–6447.

Archibald, S., Staver, A. C., and Levin, S. A. (2012). Evolution of human-driven fire regimes in africa. *Proceedings of the National Academy of Sciences*, 109(3):847–852.

Bird, M. and Cali, J. (1998). A million-year record of fire in sub-saharan africa. *Nature*, 394(6695):767.

Bontemps, S., Defourny, P., Bogaert, E. V., Arino, O., Kalogirou, V., and Perez, J. R. (2011). Globcover 2009-products description and validation report.

Brovkin, V., Claussen, M., Petoukhov, V., and Ganopolski, A. (1998). On the stability of the atmosphere-vegetation system in the sahara/sahel region. *Journal of Geophysical Research: Atmospheres*, 103(D24):31613–31624.

Fick, S. E. and Hijmans, R. J. (2017). Worldclim 2: new 1-km spatial resolution climate surfaces for global land areas. *International Journal of Climatology*, 37(12):4302–4315.

Gorelick, N., Hancher, M., Dixon, M., Ilyushchenko, S., Thau, D., and Moore, R. (2017). Google earth engine: Planetary-scale geospatial analysis for everyone. *Remote Sensing of Environment*.

Greve, M., Lykke, A. M., Blach-Overgaard, A., and Svenning, J.-C. (2011). Environmental and anthropogenic determinants of vegetation distribution across africa. *Global Ecology and Biogeography*, 20(5):661–674.

Hare, S. R. and Mantua, N. J. (2000). Empirical evidence for north pacific regime shifts in 1977 and 1989. *Progress in oceanography*, 47(2-4):103–145.

Hengl, T., Mendes de Jesus, J., Heuvelink, G. B. M., Ruiperez Gonzalez, M., Kilibarda, M., Blagotić, A., Shangguan, W., Wright, M. N., Geng, X., Bauer-Marschallinger, B., Guevara, M. A., Vargas, R., MacMillan, R. A., Batjes, N. H., Leenaars, J. G. B., Ribeiro, E., Wheeler, I., Mantel, S., and Kempen, B. (2017). SoilGrids250m: Global gridded soil information based on machine learning. *PLOS ONE*.

Hirota, M., Holmgren, M., Van Nes, E. H., and Scheffer, M. (2011). Global resilience of tropical forest and savanna to critical transitions. *Science*, 334(6053):232–235.

Hoelzmann, P., Jolly, D., Harrison, S., Laarif, F., Bonnefille, R., and Pachur, H.-J. (1998). Mid-holocene land-surface conditions in northern

africa and the arabian peninsula: A data set for the analysis of biogeo-physical feedbacks in the climate system. *Global biogeochemical cycles*, 12(1):35–51.

Huete, A. R., Didan, K., Huete, A., Didan, K., Leeuwen, W. V., Jacobson, A., Solanos, R., and Laing, T. MODIS VEGETATION INDEX (MOD 13) ALGORITHM THEORETICAL BASIS DOCUMENT Principal Investiga-tors Development Team MODIS Product ID: MOD13.

Huffman, G. J., Bolvin, D. T., Nelkin, E. J., Wolff, D. B., Adler, R. F., Gu, G., Hong, Y., Bowman, K. P., and Stocker, E. F. (2007). The trmm multisatellite precipitation analysis (tmpa): Quasi-global, multiyear, combined-sensor precipitation estimates at fine scales. *Journal of hy-drometeorology*, 8(1):38–55.

Jolly, D., Prentice, I. C., Bonnefille, R., Ballouche, A., Bengo, M., Brenac, P., Buchet, G., Burney, D., Cazet, J.-P., Cheddadi, R., et al. (1998). Biome reconstruction from pollen and plant macrofossil data for africa and the arabian peninsula at 0 and 6000 years. *Journal of Biogeogra-phy*, 25(6):1007–1027.

Knowlton, N. (1992). Thresholds and multiple stable states in coral reef community dynamics. *American Zoologist*, 32(6):674–682.

Lehmann, C. E., Archibald, S. A., Hoffmann, W. A., and Bond, W. J. (2011). Deciphering the distribution of the savanna biome. *New Phytologist*, 191(1):197–209.

Leutner, B. and Horning, N. (2016). Rstoolbox: tools for remote sensing data analysis. *R package version 0.1*, 4.

Majumder, S., Tamma, K., Ramaswamy, S., and Guttal, V. (2017). Inferring critical points of ecosystem transitions from spatial data. *bioRxiv*, page 187799.

Markham, C. G. (1970). Seasonality of Precipitation in the United States. *Source: Annals of the Association of American Geographers*, 60(3):593–597.

Murphy, B. P. and Bowman, D. M. (2012). What controls the distribution of tropical forest and savanna? *Ecology letters*, 15(7):748–758.

Nes, E. H., Hirota, M., Holmgren, M., and Scheffer, M. (2014). Tipping points in tropical tree cover: linking theory to data. *Global change biology*, 20(3):1016–1021.

Oliveras, I. and Malhi, Y. (2016). Many shades of green: the dynamic tropical forest–savannah transition zones. *Phil. Trans. R. Soc. B*, 371(1703):20150308.

Rietkerk, M., Ketner, P., Burger, J., Hoorens, B., and Olff, H. (2000). Multiscale soil and vegetation patchiness along a gradient of herbivore impact in a semi-arid grazing system in west africa. *Plant Ecology*, 148(2):207–224.

Sanderson, E. W., Jaiteh, M., Levy, M. A., Redford, K. H., Wannebo, A. V., and Woolmer, G. (2002). The human footprint and the last of the wild. *BioScience*, 52(10):891–904.

Scheffer, M., Carpenter, S., Foley, J. A., Folke, C., and Walker, B. (2001). Catastrophic shifts in ecosystems. *Nature*, 413(6856):591–596.

Scheffer, M., Hosper, S., Meijer, M., Moss, B., and Jeppesen, E. (1993). Alternative equilibria in shallow lakes. *Trends in ecology & evolution*, 8(8):275–279.

Scheiter, S., Higgins, S. I., Beringer, J., and Hutley, L. B. (2015). Climate change and long-term fire management impacts on australian savannas. *New phytologist*, 205(3):1211–1226.

Staal, A., Dekker, S. C., Xu, C., and van Nes, E. H. (2016). Bistability, spatial interaction, and the distribution of tropical forests and savannas. *Ecosystems*, 19(6):1080–1091.

Staver, A. C., Archibald, S., and Levin, S. (2011a). Tree cover in sub-saharan africa: rainfall and fire constrain forest and savanna as alternative stable states. *Ecology*, 92(5):1063–1072.

Staver, A. C., Archibald, S., and Levin, S. A. (2011b). The global extent and determinants of savanna and forest as alternative biome states. *Science*, 334(6053):230–232.

Team, R. C. (2000). R language definition. *Vienna, Austria: R foundation for statistical computing*.

Venter, O., Sanderson, E. W., Magrach, A., Allan, J. R., Beher, J., Jones, K. R., Possingham, H. P., Laurance, W. F., Wood, P., Fekete, B. M., et al. (2016). Sixteen years of change in the global terrestrial human footprint and implications for biodiversity conservation. *Nature Communications*, 7:12558.

Wuyts, B., Champneys, A. R., and House, J. I. (2017). Amazonian forest-savanna bistability and human impact. *Nature Communications*, 8:15519.